

Retinex-Diffusion: On Controlling Illumination Conditions in Diffusion Models via Retinex Theory

Xiaoyan Xing¹, Vincent Tao Hu^{3*}, Jan Hendrik Metzen²
Konrad Groh², Sezer Karaoglu¹, Theo Gevers¹

1. UvA-Bosch Delta Lab 2. Bosch Center for Artificial Intelligence 3. LMU Munich



Figure 1. Motivated by the recent state-of-the-art image manipulation method [9] can not handle the low-level manipulation, such as relighting the scene, or creating illumination effect (top row). We present physics-guided and training-free diffusion for controlling illumination conditions in images. In image synthesis, our method generates photo-realistic illumination conditions under the proper illumination property guidance. Our model is also able to perform illumination editing of the original images, such as adding new illumination to images or face relighting (bottom row). Our approach is training-free and easily integrated with most pixel-based diffusion models, enhancing their illumination control capabilities efficiently.

Abstract

This paper introduces a novel approach to illumination manipulation in diffusion models, addressing the gap in conditional image generation with a focus on lighting conditions. We conceptualize the diffusion model as a black-box image render and strategically decompose its energy function in alignment with the image formation model. Our method effectively separates and controls illumination-related properties during the generative process. It generates images with realistic illumination effects, including cast shadow, soft shadow, and inter-reflections. Remark-

ably, it achieves this without the necessity for learning intrinsic decomposition, finding directions in latent space, or undergoing additional training with new datasets.

1. Introduction

Generative models have shown their ability to create images that closely resemble real ones. The advent of conditional diffusion models has further enhanced the generation of specific semantic content [11, 16, 24, 27, 35], contents [9, 20, 34, 38], layout [19, 50], etc. However, a notable limitation is their inability to control illuminations precisely

*Work was done at University of Amsterdam.

in the generated images. On the other hand, physically-based rendering pipelines like Blender [10] can achieve high-fidelity illumination but are time-consuming and lack diversity. In this paper, we combine the generative capabilities of diffusion models with the guidance of physically-based models to create a novel approach for controlling illumination conditions in both generated and real images.

Altering illumination conditions is essential for various computer vision and computer graphics tasks. Typically, this involves decomposing and recomposing the intrinsic components of a scene [14, 30, 31, 33, 36, 52]. Recently, the advancement of the generative models provide a way to solve such tasks end-to-end, e.g., finding the corresponding direction in the Style-GAN’s latent space [6, 7]. However, these methods often require extensive datasets containing various intrinsic labels such as surface normals, depth, light sources, or the direction searching. In contrast, we propose a more straightforward approach to illumination condition control by harnessing the power of diffusion models guided by physical principles (Table 1).

In this paper, we propose harnessing the generative process of the diffusion model as a self-contained rendering pipeline, enabling the manipulation of illumination conditions through physics-driven guidance. This approach allows us to circumvent the intricate tasks of decomposing and recomposing scene intrinsic components. Consequently, it can be seamlessly applied to diverse datasets and lighting scenarios without the need for additional training, tuning, or extra data labels.

In summary, the contributions are as follows:

- We regard the diffusion model as a black-box image render and decompose its energy function according to the image formation model.
- We introduce illumination-controllable image synthesis and geometry-preserving real image relighting, both guided by physics-based principles.
- Our work provides photorealistic control of illumination in both generated and real images, delivering results that are on par with, and in some aspects surpass, models tailored to specific data domains.
- Our approach is entirely devoid of training requirements and does not rely on any CGI techniques to attain controllable illumination conditions.

2. Related work

Conditional Diffusion Models. Diffusion models perform well in various tasks due to their controllability [50]. This includes image content [34], image layout [38], audio content [32], and human motion generation [45]. However, current diffusion models often struggle with fine-grained control over illumination as illustrated in Figure 1. Our work leverages the knowledge of illumination to formulate flexible energy functions. Classifier-guidance [13] demonstrates

that diffusion models can be guided by pretraining a noisy-data based classifier. Classifier-free guidance [17] further eliminates the need for extra pretraining by randomly dropping out the guidance signal during training. Self-guided diffusion models [19] even remove the annotation process altogether. More recently, ControlNet [50] and its variants has been used to address the illumination condition in diffusion models [25, 48], yet those methods usually require training Controlnet on extra dataset, resulting in a complex and costly implementation.

Our method is complementary to all these approaches. To fully leverage the potential of pretrained diffusion models, we propose an additional energy function based on illumination theory to guide the generation of the diffusion models.

Diffusion Based Image manipulation. A substantial body of literature is dedicated to image manipulation and editing using diffusion models [9, 16, 24, 34, 35]. While these methods harness the remarkable generative capabilities of diffusion models to modify high to mid-level image attributes such as semantics [18, 27] and layouts [38, 50], the control of lower-level features, especially illumination, has been unexplored. To this end, we introduce a novel illumination manipulation method tailored for conditional image generation based on illumination. Our approach involves decomposing the illumination-related properties during the generative process and applying targeted guidance based on these properties.

Notably, our training-free method can be easily integrated into major diffusion models, enhancing their ability to adjust illumination conditions on-the-fly. This contrasts with [36], which is limited to human faces and relies on trained and pre-trained parameters.

Intrinsic Image Decomposition. Intrinsic image decomposition methods [2–5, 12, 21, 29, 31, 33, 46, 51, 52] aim to decompose an image into illumination-relevant and illumination-irrelevant parts. Recent diffusion-based methods [26, 49] have shown impressive decomposition results, indicating that diffusion models have an awareness of intrinsic.

Our method builds on one of the earliest vision techniques, retinex theory [28], for solving intrinsic decomposition. It extracts the illumination property of the image and approximates it as the illumination-irrelevant component of the image at a very low cost. We employ the simple decomposition results as hints to guide the pre-trained diffusion models to generate images with designated illumination.

3. Preliminaries

To illustrate the challenges in modifying illumination attributes within diffusion models, we begin by comparing the image synthesis process of diffusion models with the image formation of real-world images.

	Neural rendering[31, 52]	Directional search [6, 7]	DiFaReli [36]	Ours
Neural backbone	CNN, Transformer	Style-GAN	Diffusion	Diffusion
label-free	light mask, depth	✓	light source, cam paras	✓
End to End	×	✓	×	✓
Different types of data	×	×	×	✓
Diverse outputs	×	Some of them	×	✓

Table 1. Comparison with previous illumination control methods.

3.1. Real-world Image Formation

The image formation can be modelled by [40]:

$$I = m(\mathbf{n}, \mathbf{l}) \int_{\omega} f_c(\lambda) e(\lambda) \rho(\lambda) d\lambda \quad (1)$$

where \mathbf{n} represents the surface normal vector, and \mathbf{l} denotes the direction of the light source. The term m represents the geometric relationship in the interaction. Additionally, λ indicates the wavelength, $f_c(\lambda)$ the camera spectral sensitivity, $e(\lambda)$ the spectral power distribution of the illuminant, ρ the surface reflectance.

Assuming the sensor response is linear and the wavelength of visible spectrum is narrow (λ_I), Equation (1) is simplified as:

$$I = m(\mathbf{n}, \mathbf{l}) e(\lambda_I) \rho(\lambda_I). \quad (2)$$

Then, at point \mathbf{x} on the surface, the decomposition of $I(\mathbf{x})$ can be approximated by:

$$I(\mathbf{x}) = R(\mathbf{x}) \odot S(\mathbf{x}), \quad (3)$$

where \odot represents the Hadamard product, $R(\mathbf{x})$ is the reflectance, which is illumination-invariant, and $S(\mathbf{x})$ is the shading, which is illumination-variant. By manipulating shading, one can control the illumination properties in a physics-based manner.

3.2. Diffusion Image Generation

Diffusion models [18, 41, 44] gradually perturb data using a forward diffusion process and then reverse the process to reconstruct the original data, as explained in previous studies [1, 13, 18, 43]. Let $q(\mathbf{x}_0)$ denote the unknown data distribution in \mathbb{R}^D . The forward diffusion process, indexed by time t as $\{\mathbf{x}_t\}_{t \in [0, T]}$, can be succinctly represented by the following forward Stochastic Differential Equation (SDE):

$$d\mathbf{x} = \mathbf{f}(\mathbf{x}, t)dt + g(t)d\mathbf{w}, \quad (4)$$

where $\mathbf{w} \in \mathbb{R}^D$ is a standard Wiener process, $\mathbf{f}(\cdot, t) : \mathbb{R}^D \rightarrow \mathbb{R}^D$ is the drift coefficient and $g(t) \in \mathbb{R}$ is the diffusion coefficient. The $\mathbf{f}(\mathbf{x}, t)$ and $g(t)$ are related to the noise size and determine the perturbation kernel $q_{t|0}(\mathbf{x}_t|\mathbf{x}_0)$ from time 0 to t .

Let $q_t(\mathbf{x})$ be the marginal distribution of the SDE at time t in Equation (4). Its time reversal can be described by another SDE [44]:

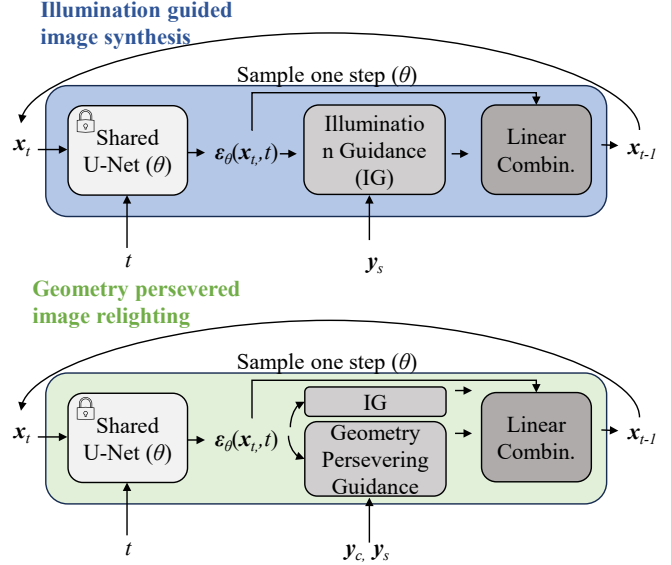


Figure 2. Overall diagram of the proposed illumination control diffusion method. Top, the illumination guidance image generation; Bottom, image relighting. x_t represents the image at time step t , ϵ_θ is the pre-trained U-Net [39]. y_s and y_c are prompts for illumination guidance and the geometry persevering guidance.

$$d\mathbf{x} = [\mathbf{f}(\mathbf{x}, t) - g(t)^2 \mathbf{s}(\mathbf{x}, t)]dt + g(t)d\bar{\mathbf{w}}, \quad (5)$$

where $\bar{\mathbf{w}}$ is a reverse-time standard Wiener process with dt as an infinitesimal negative timestep, and $\mathbf{s}(\mathbf{x}, t) = \nabla_{\mathbf{x}} \log q_t(\mathbf{x})$ represents the score. The score, similar to energy, allows us to introduce an additional energy function $\mathcal{E}(\cdot, \cdot, \cdot)$ into the reverse SDE process for the specific guidance. We will further discuss the design of the energy function for illumination-based guidance in later sections.

4. Method

As illustrated in Figure 2, our method performs two tasks: 1) it can control the illumination conditions of the generated image, and 2) it can apply new lighting conditions on real images. To accomplish these tasks, we first reformulate the energy function in the diffusion process. Then, we introduce the illumination guidance in image synthesis. Finally, we propose geometry persevered relighting for real images. Notably, this pipeline requires no further training, nor extra data labels or CGI techniques.

4.1. Illumination Energy Decomposition

We reconsider the reversed SDE processing of diffusion image generation based on the image formation model. As mentioned in the preliminary, an image can be decomposed into illumination-variant I and illumination-invariant

R parts. Therefore, we decompose the energy function $\mathcal{E}(\mathbf{y}, \mathbf{x}, t)$ by the sum of two log potential functions [8]:

$$\begin{aligned}\mathcal{E}(\mathbf{y}, \mathbf{x}, t) &= \lambda_I \mathcal{E}_I(\mathbf{y}, \mathbf{x}, t) + \lambda_R \mathcal{E}_R(\mathbf{y}, \mathbf{x}, t) \\ &= \lambda_I \mathbb{E}_{q_{t|0}(\mathbf{x}_t|\mathbf{x})} \mathcal{S}_I(\mathbf{y}, \mathbf{x}_t, t) \\ &\quad + \lambda_R \mathbb{E}_{q_{t|0}(\mathbf{x}_t|\mathbf{x})} \mathcal{S}_R(\mathbf{y}, \mathbf{x}_t, t),\end{aligned}\tag{6}$$

where \mathbf{y} is our target guidance for energy, $\mathcal{E}_I(\cdot, \cdot, \cdot) : \mathbb{R}^D \times \mathbb{R}^D \times \mathbb{R} \rightarrow \mathbb{R}$ and $\mathcal{E}_R(\cdot, \cdot, \cdot) : \mathbb{R}^D \times \mathbb{R}^D \times \mathbb{R} \rightarrow \mathbb{R}$ are the log potential functions, \mathbf{x}_t is the perturbed source image in the forward SDE, $q_{t|0}(\cdot|\cdot)$ is the perturbation kernel from time 0 to time t in the forward SDE, $\mathcal{S}_I(\cdot, \cdot, \cdot) : \mathbb{R}^D \times \mathbb{R}^D \times \mathbb{R} \rightarrow \mathbb{R}$ and $\mathcal{S}_R(\cdot, \cdot, \cdot) : \mathbb{R}^D \times \mathbb{R}^D \times \mathbb{R} \rightarrow \mathbb{R}$ are functions measuring similarity between the target guidance and perturbed source image. $\lambda_R \in \mathbb{R} > 0$ and $\lambda_S \in \mathbb{R} > 0$ are weighting hyper-parameters for illumination-variant and illumination-invariant components, respectively.

In the reverse process, given by Equation (5), and adopting a step size of h , the iteration rule from s to $t = s - h$ is as follows when applying our new illumination-based energy function:

$$\begin{aligned}\mathbf{x}_t &= \mathbf{x}_s - [\mathbf{f}(\mathbf{x}, s) - g(s)^2(\mathbf{s}(\mathbf{x}_s, s) - \nabla_{\mathbf{x}} \mathcal{E}(\mathbf{y}, \mathbf{x}, s))]h \\ &\quad + g(s)\sqrt{h}\mathbf{z},\end{aligned}\tag{7}$$

where $\mathbf{z} \sim \mathcal{N}(\mathbf{0}, \mathbf{I})$. The expectation in $\mathcal{E}(\mathbf{y}, \mathbf{x}, s)$ is estimated by the Monte Carlo method of a single sample for efficiency. In the following section, we will introduce the construction of the energy function based on related illumination theories.

4.2. Illumination-Energy Guided Generation

Prompt for Illumination Energy Illumination is related to the brightness of a pixel. [36] shows that by matching the mean value difference between the reversed sampling and generated sampling, the consistency of global brightness of human portrait can be realized. This can be explained by Equation (3), where the reflectance R of the human portrait can be approximated as a constant. Therefore, the intensity of pixel is directly reflecting illumination S . However, this simplification falls short when dealing with more complex surface reflectance. Therefore, an additional step of illumination property extraction is required.

We modify the multi-scale retinex model [37] to extract illumination properties. The illumination is computed from the denoised image x_t at the candidate step t . First $x_t \in \mathbb{R}^{H \times W \times 3}$ is filtered by 2D Gaussians at multiple scales, to capture the image’s varying level of geometry and illumination. Subsequently, these blurred images are combined using either uniform or user-defined weights. The

processing is formed as:

$$f_s(m_t, n_t) = \sum_{r,g,b} \sum_{k=1}^N w_k \cdot \left(\frac{1}{2\pi\sigma_k^2} e^{-\frac{i^2+j^2}{2\sigma_k^2}} * x_t(m, n) \right),\tag{8}$$

where $f_s(m_t, n_t)$ is the estimated lighting at pixel (m, n) at given timestep t , $\{i, j\}$ represents the position of the Gaussian center, σ_k is the standard deviation for the k^{th} scale, and $*$ donates the convolution.

Illumination Energy Guidance We model the target illumination condition by parameterizing the illumination map as a composition of N 2D Gaussian functions $G(\cdot)$ as:

$$y_s = \sum_{i=1}^N \alpha_i G(\mu_i, \Sigma_i),\tag{9}$$

where its mean μ_i represents the position of the light source (for the visible light source) or the location of the brightest parts of the image (for the invisible light source), and its covariance matrix (Σ_i) describes the spread and directionality of the light. α_i is the weight of corresponding Gaussian, which is subject to $\sum \alpha_i = 1$.

After the illumination property $f_s(\cdot)$ and the illumination prompt y_s are computed, their difference can be quantified using any differentiable similarity metric. In practice, the pixel-wise mean square error is used to calculate this difference, which is defined as:

$$\mathcal{S}_I(y_s, \mathbf{x}, t) = \sum_{\mathbf{x} \in \mathbf{x}} \|f_s(x_t) - y_s\|_2.\tag{10}$$

4.3. Illumination-Energy on Real-world Image

The illumination-based guidance generation can be extended to modify or add lighting conditions in real-world images, as shown in Figure 2. This involves two key steps: firstly, an inverse processing stage to convert the input image into a latent code, and secondly, a reflectance-based correction to maintain the original image geometry while altering the lighting. This approach enables flexible lighting manipulation while preserving the original image’s core structure and details.

Real-image inversion Given an input image $x_0 \in \mathbb{R}^{H \times W \times 3}$, we utilize the inverse process of DDIM [42] converts it to a latent $x_z \in \mathbb{R}^{H \times W \times 3}$ at the final forward DDIM step z . Hence, given x_z as input, the illumination-guided generative process is able to change the light condition of the real image. Yet, the edited image may not have the exact same geometry, since the guidance on shading may also disturb the geometry.

Geometry persevering guidance Another key contribution of our method is the reflectance-based correction for preserving the geometry of the edited image. Similar to the condition on the illumination property, the geometry property can be regarded as part of illumination-invariant component R . And it can be represented as the surface reflectance difference. We apply a gradient-based method to extract such difference by calculating the cross color ratios (CCR) [15] of the surface.

Given an image $x_0 \in \mathbb{R}^{H \times W \times 3}$ to be edited and two neighbouring pixels p_1, p_2 . The CCR’s are calculated as:

$$M_{RG} = \frac{R_{p_1} G_{p_2}}{R_{p_2} G_{p_1}}, M_{RB} = \frac{R_{p_1} B_{p_2}}{R_{p_2} B_{p_1}}, M_{GB} = \frac{G_{p_1} B_{p_2}}{G_{p_2} B_{p_1}}, \quad (11)$$

where, M_{RG}, M_{RB} and M_{GB} are the CCR for the color channel pairs (R, G) , (R, B) and (G, B) , respectively. To simplify the writing, we use M_{RG} to represent the CCR for all channel pairs, in the following statements. Given the image formation in Equation (2), and the illumination condition are close in a small neighborhood [12], we obtain:

$$\begin{aligned} \log M_{RG} &= \log(\rho^{R_{p_1}}) + \log(\rho^{G_{p_2}}) \\ &\quad - \log(\rho^{R_{p_2}}) - \log(\rho^{G_{p_1}}). \end{aligned} \quad (12)$$

Therefore, the CCR are illumination invariant and only depends on reflectance transitions. For more mathematical details, please refer to the supplementary material section. The final normalized target CCR matrix $\mathbf{C}_{x_0} \in \mathbb{R}^{H \times W \times 3}$ is $[M_{RG}, M_{RB}, M_{GB}]$. The operation to compute the CCR matrix for a image is expressed as: $f_c(\cdot)$.

Similarly, the CCR matrix of the generated image at time step t can be also calculated in the same manner, denoted by $\mathbf{C}_{x_t} = f_c(x_t)$.

In a manner similar to the illumination prompting, we define the geometry-related prompt as y_c . Hence, the discrepancy between the target CCR y_c and the computed CCR $f_c(x_t)$ at sampling step t is quantified as follows:

$$\mathcal{S}_R(y_c, \mathbf{x}_t, t) = \sum_{x \in \mathbf{x}} \|f_c(x_t) - y_c\|_2. \quad (13)$$

Then, the anti-gradient of the reflectance difference $-\nabla_{\mathbf{C}_t} \mathcal{L}$ is sent to the diffusion process together with the anti-gradient of the illumination difference $-\nabla_{S_t} \mathcal{L}$, to achieve the geometry preserved relighting in the real image editing.

5. Experiments

Pre-trained diffusion models. Our approach leverages the generative capabilities of pre-trained diffusion models. A summary of the models used in our study, along with the datasets on which they are pre-trained, is as follows:

- **ADM** [13]: pretrained on LSUN-Bedroom[47] for generating and editing the diverse illumination conditions of bedrooms.

- **EDM** [23]: pretrained on FFHQ dataset for generating diverse illumination conditions of human faces.
- **DDIM** [42]: pretrained on CelebA-HQ [22] for editing illumination conditions of human faces.

5.1. Illumination Guidance in Image Synthesis

First, we demonstrate the effectiveness of our method in generating photo-realistic images with different illumination variants, including different light direction, shadow, and strength of illumination. Then, we evaluate the illumination guidance by comparing it with the human-instructed image to image generative model [9]. In the case of the human-instructed model, we employ text prompts that specify fixed illumination conditions to generate images. In contrast, our method directly integrates illumination prompts to guide the generation process.

Figure 3 and Figure 5 illustrate the images generated under varying illumination condition guidance. The associated illumination features are displayed alongside the images. The results showcase the photo-realistic generation of illumination conditions, such as turning on a lamp or increasing outdoor illumination, and so on.

Figure 4 highlights our method’s application in controlling the illumination effect of a new light source. By using consistent illumination direction prompts, it illustrates the ability to produce a range of illumination effects. These variations correspond to the intensity of the light source, illustrating the flexibility of our method in adjusting light intensity within a scene.

Figure 6 visually demonstrates the results of increasing the illumination coming from the window. These results can be compared with those obtained using human-guided image-to-image generative methods, Instruct-Pix2Pix [9], which struggles on generating the image with the prompted illumination, our method generates vivid illumination with our illumination guided generation. The hyper-parameters of [9] are carefully selected to obtain the stable results.

Table 2 presents the quantitative evaluation of our method for generating images under specified illumination conditions. We use MSE as the metric to measure the discrepancy between the illumination extracted from the generated images and the given illumination prompt. Across three distinct illumination conditions, our method consistently achieves a better MSE score compared to the baseline method without guidance and [9] with our carefully designed prompt, underscoring the effectiveness of ours.

5.2. Illumination Editing in Real-world Image

We further evaluate our methods on illumination editing in synthetic and real-world images. Figure 7 demonstrates our method’s capability in illumination editing on various images. The sequence comprises the original input image, its inversion, and the final relighted image, each accompa-

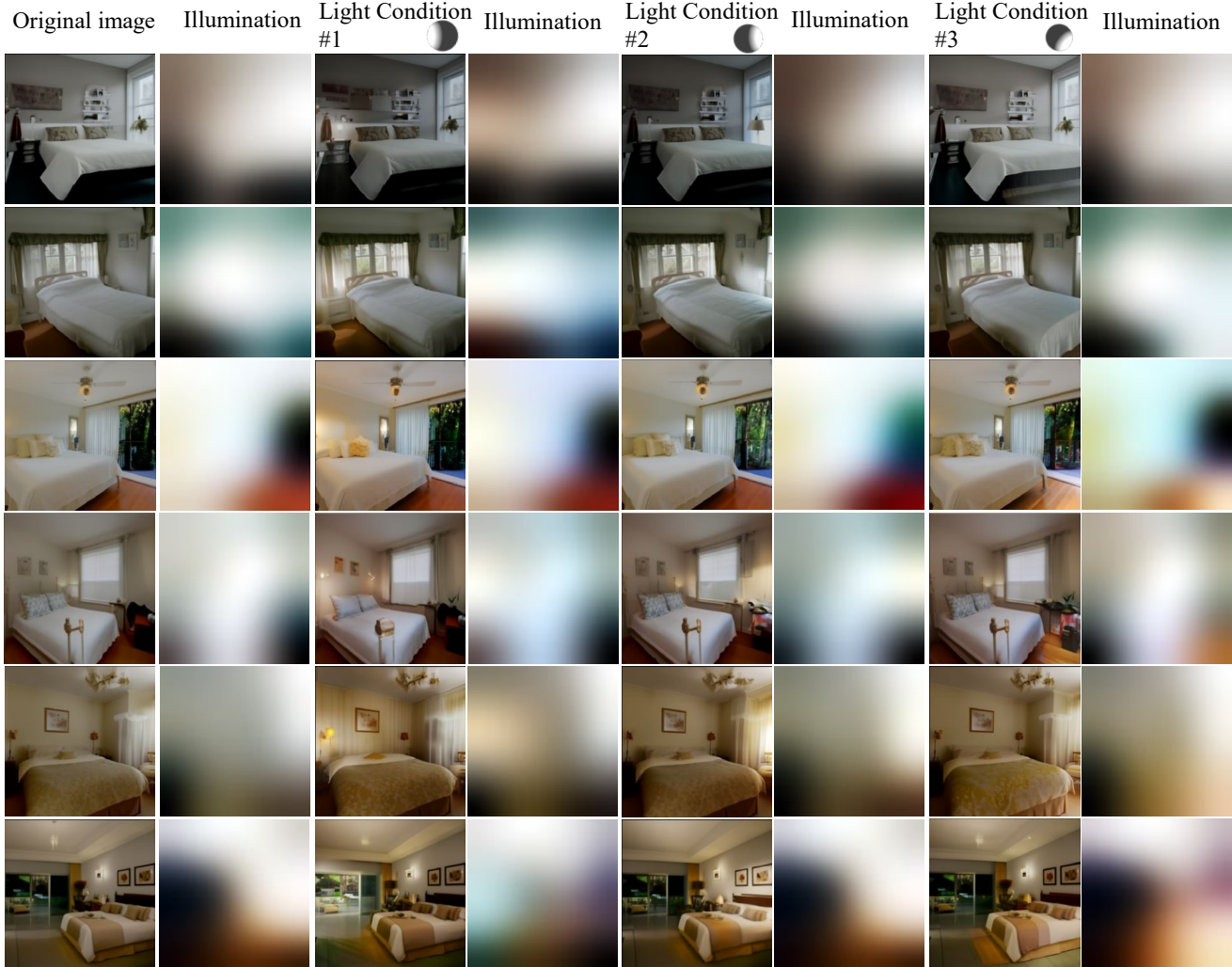


Figure 3. Illumination Property-Guided Image Generation: Each pair of columns displays the generated image alongside its corresponding illumination feature. The initial two columns show the original image without illumination guidance and its illumination feature. Subsequent columns illustrate images generated under various specific lighting conditions, with the illumination direction indicated by a sphere.

	Illumination condition #1	Illumination condition #2	Illumination condition #3
Instruct-Pix2Pix [9]	0.0896	0.0835	0.0346
ADM [13]	0.0887	0.0823	0.0344
Ours (ADM+illum. guided)	0.0757	0.0706	0.0311

Table 2. Quantitative results of the illumination map generated by Instruct-Pix2Pix[9](w. text prompt guidance), ADM (w/o. illumination guidance) and ours (w. illumination guidance).

nied by their corresponding illumination features. Remarkably, our method skillfully adjusts the illumination direction while maintaining the original geometry, showcasing its effectiveness even on colorful surfaces.

Figure 8 shows real-world image relighting using our

method, which operates without learned intrinsics [31] or directional searches in latent space [6]. The loss of high-frequency detail is attributed to the limitations of DDIM inversion, as our guidance does not significantly alter the geometry.

Figure 9 showcases our real-face relighting results. Our method surpasses the performance of the state-of-the-art image-to-image manipulation method by [9] (we carefully designed their text prompt.). Additionally, our results are comparable to those obtained by the specialized face relighting method of [36].

5.3. Ablation Study & Discussion

Illumination property extraction. As introduced in Section 4.2, by extracting the illumination property, one can

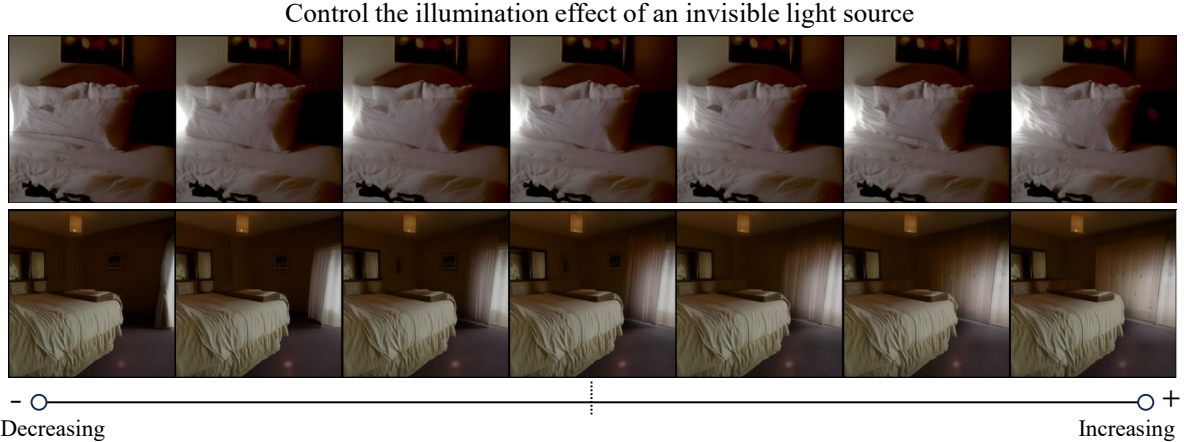


Figure 4. Illumination effect control of an invisible light source. Given the same illumination direction prompt, our method is able to generate multiple variants of illumination effect with respect to the strength of the light source.



Figure 5. Illumination Property-Guided Image Generation (Using EDM [23]): Each pair of columns displays the generated image alongside its corresponding illumination feature. Illumination direction indicated by a sphere.

distinguish the illumination condition from the composited image generation. Here, we evaluate the illumination guidance without extracting the illumination property. As shown in Figure 10, we guide the image synthesis process based on the same illumination prompts, while we gradually increase the lighting range of the light prompts, the content of the image guided by the non-illumination specific property shifts rapidly. Also, images are much blurry compared to the ones with extracting illumination properties. Such results clearly showcase the effectiveness of the illumination property extraction.

Computational efficiency. The computational cost analysis of our method (Table 3), reveals minimal additional burden on the guided diffusion model. Specifically, the inference time for image generation/editing, using standard resolutions, batch sizes, and sampling steps, shows only a



Figure 6. Visual comparison with state-of-the-art image to image diffusion model [9] in the context of generating new lighting conditions.

Sampler	Batch Size	Sampling steps	Batch Time (s) w/o. guidance	Batch Time (s) w. guidance
ADM [13]	16	100	102.63	110.85
DDIM [42]	8	40	11.59	15.63
EDM [23]	64	15	4.17	4.35

Table 3. Comparison of generation times (per batch) with and without illumination guidance using ADM [13], DDIM [42], and EDM [23] on a Pytorch framework. Tests were conducted on an Nvidia RTX4090 GPU.

marginal increase. An increment of 8.2 seconds is shown for ADM [13], 0.17 seconds for EDM [23], and 4.04 seconds for DDIM [42], affirming the efficiency of ours.

Other intrinsic decomposition methods. Theoretically, the retinex model can be replaced by any other decomposition models, including learning-based models. We em-

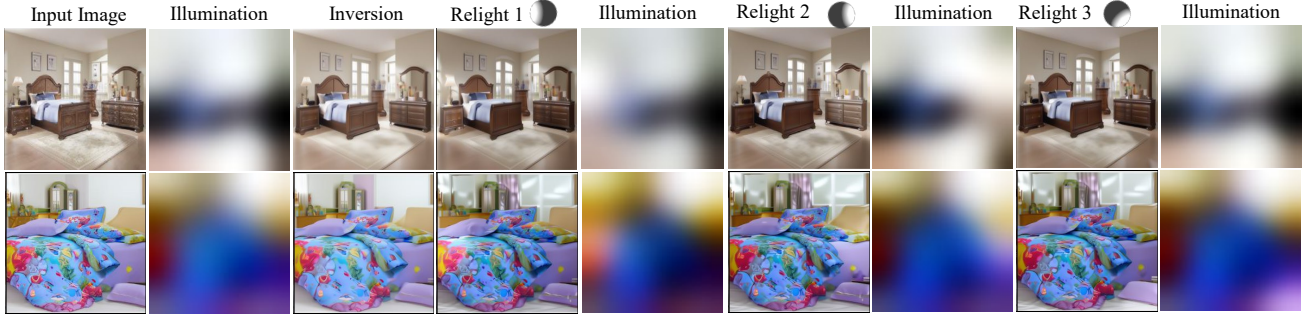


Figure 7. Geometry-Preserved Image Relighting: The sequence from left to right displays the original input image, the inverted image, and the image relighting results under three different lighting conditions (denoted as Relight 1, Relight 2, and Relight 3). This progression demonstrates the effectiveness of our method in maintaining geometric consistency while altering illumination conditions. Illumination direction indicated by a sphere.



Figure 8. Real indoor image relighting comparison: The left column displays real images captured with invisible light turned on and off, illustrating the ground truth. The middle-left column showcases images relighted by the method proposed by Li et al. [31], which utilizes multiple sub-networks for intrinsic decomposition and generates new images based on these modified intrinsics. The middle-right column shows StylitGAN’s [6] relighting, applying directional search in the latent space. The right column presents our results using illumination-guided diffusion, notably achieving relighting without learned intrinsic decomposition, directional search, or CGI techniques.

ploy the multiscale retinex model for following reason: 1) it is naturally differentiable, and can be directly used to calculate the score; 2) it is computational cheap, since it only contains few convolution operations, it will not significantly increase the sampling time.

6. Conclusion

We proposed a novel and physics-based, training-free method for manipulating illumination in both diffusion-generated and real images. Our method realizes accurate illumination-conditioned image generation by reforming the energy function of diffusion models based on the image formation model. Our approach does not require any type of extra training or direction research. It is easy to

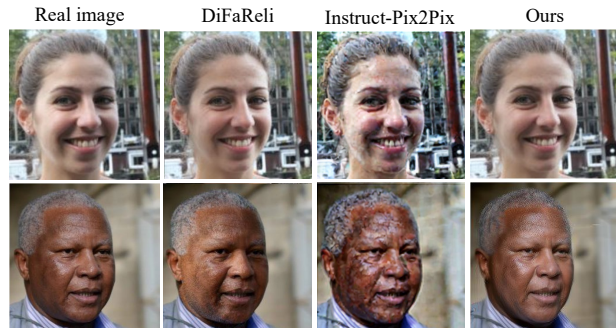


Figure 9. Real face image relighting comparison: The left column presents the real face image for relighting. Middle-left column, the latest diffusion based face relighting method [36], which is conditioned on multiple intrinsic and extrinsic components, and needs multiple pretrained methods to decompose those components. Middle-right column, human instructed image to image generative method [9], fails badly on relighting. Right column, our method is able to relight the face without learned intrinsic decomposition, directional search, or CGI techniques.

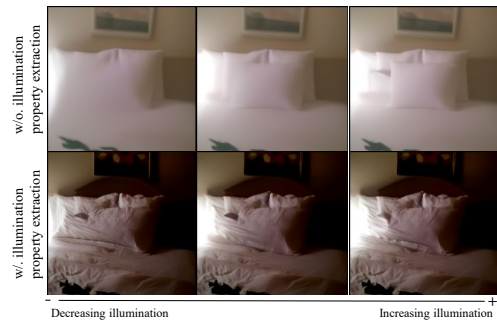


Figure 10. Ablation comparison of the illumination property extraction. Top row: illumination guided generation without extracting the illumination property. Bottom row: illumination guided generation with the extracted illumination property.

be embedded into current diffusion models. By prompting the illumination-related feature, the diffusion model is able to generate/adjust illumination-related semantics for proper illumination conditions, such as turning on the lamp and opening the window.

Limitation. Such illumination control is not always accurate, and it is aligned to the learned data distribution of pretrained diffusion models. A deeper investigation on extracting intrinsics of the diffusion models is needed in the future.

References

- [1] Fan Bao, Chongxuan Li, Jun Zhu, and Bo Zhang. Analytic-dpm: an analytic estimate of the optimal reverse variance in diffusion probabilistic models. In *International Conference on Learning Representations*, 2021. 3
- [2] Jonathan T Barron and Jitendra Malik. Shape, illumination, and reflectance from shading. *IEEE TPAMI*, 37(8):1670–1687, 2015. 2
- [3] Anil S Baslamisli, Thomas T Groenestegge, Partha Das, Hoang-An Le, Sezer Karaoglu, and Theo Gevers. Joint learning of intrinsic images and semantic segmentation. In *ECCV*, 2018.
- [4] Anil S Baslamisli, Hoang-An Le, and Theo Gevers. Cnn based learning using reflection and retinex models for intrinsic image decomposition. In *CVPR*, 2018. 1
- [5] Anil S Baslamisli, Partha Das, Hoang-An Le, Sezer Karaoglu, and Theo Gevers. Shadingnet: Image intrinsics by fine-grained shading decomposition. *IJCV*, 129(8):2445–2473, 2021. 2
- [6] Anand Bhattad and David A Forsyth. Stylitgan: Prompting stylegan to produce new illumination conditions. *arXiv preprint arXiv:2205.10351*, 2022. 2, 3, 6, 8
- [7] Anand Bhattad, Viraj Shah, Derek Hoiem, and DA Forsyth. Make it so: Steering stylegan for any image inversion and editing. *arXiv preprint arXiv:2304.14403*, 2023. 2, 3
- [8] Christopher M. Bishop. *Pattern Recognition and Machine Learning*. 2006. 4
- [9] Tim Brooks, Aleksander Holynski, and Alexei A Efros. Instructpix2pix: Learning to follow image editing instructions. In *CVPR*, pages 18392–18402, 2023. 1, 2, 5, 6, 7, 8
- [10] Blender Online Community. *Blender - a 3D modelling and rendering package*. Blender Foundation, Stichting Blender Foundation, Amsterdam, 2018. 2
- [11] Guillaume Couairon, Jakob Verbeek, Holger Schwenk, and Matthieu Cord. Diffedit: Diffusion-based semantic image editing with mask guidance. In *ARXIV*, 2022. 1
- [12] Partha Das, Sezer Karaoglu, and Theo Gevers. Pie-net: Photometric invariant edge guided network for intrinsic image decomposition. In *CVPR*, 2022. 2, 5
- [13] Prafulla Dhariwal and Alexander Nichol. Diffusion models beat gans on image synthesis. *NeurIPS*, 34:8780–8794, 2021. 2, 3, 5, 6, 7
- [14] David Futschik, Kelvin Ritland, James Vecore, Sean Fanello, Sergio Orts-Escolano, Brian Curless, Daniel Šykora, and Rohit Pandey. Controllable light diffusion for portraits. In *CVPR*, pages 8412–8421, 2023. 2
- [15] Theo Gevers and Arnold WM Smeulders. Color-based object recognition. *Pattern recognition*, 32(3):453–464, 1999. 5
- [16] Amir Hertz, Ron Mokady, Jay Tenenbaum, Kfir Aberman, Yael Pritch, and Daniel Cohen-Or. Prompt-to-prompt image editing with cross attention control. *arXiv preprint arXiv:2208.01626*, 2022. 1, 2
- [17] Jonathan Ho and Tim Salimans. Classifier-free diffusion guidance. In *NeurIPS Workshop*, 2021. 2
- [18] Jonathan Ho, Ajay Jain, and Pieter Abbeel. Denoising diffusion probabilistic models. *NeurIPS*, 2020. 2, 3
- [19] Vincent Tao Hu, David W Zhang, Yuki M. Asano, Gertjan J. Burghouts, and Cees G. M. Snoek. Self-guided diffusion models. In *CVPR*, 2023. 1, 2
- [20] Inbar Huberman-Spiegelglas, Vladimir Kulikov, and Tomer Michaeli. An edit friendly ddpm noise space: Inversion and manipulations. *arXiv*, 2023. 1
- [21] Michael Janner, Jiajun Wu, Tejas D Kulkarni, Ilker Yildirim, and Josh Tenenbaum. Self-supervised intrinsic image decomposition. In *NIPS*, 2017. 2
- [22] Tero Karras, Samuli Laine, and Timo Aila. A style-based generator architecture for generative adversarial networks. In *CVPR*, 2019. 5
- [23] Tero Karras, Miika Aittala, Timo Aila, and Samuli Laine. Elucidating the design space of diffusion-based generative models. In *NeurIPS*, 2022. 5, 7
- [24] Gwanghyun Kim, Taesung Kwon, and Jong Chul Ye. Diffusionclip: Text-guided diffusion models for robust image manipulation. In *CVPR*, 2022. 1, 2
- [25] Peter Kocsis, Julien Philip, Kalyan Sunkavalli, Matthias Nießner, and Yannick Hold-Geoffroy. Lightit: Illumination modeling and control for diffusion models. In *CVPR*, 2024. 2
- [26] Peter Kocsis, Vincent Sitzmann, and Matthias Nießner. Intrinsic image diffusion for single-view material estimation. In *CVPR*, 2024. 2
- [27] Mingi Kwon, Jaeseok Jeong, and Youngjung Uh. Diffusion models already have a semantic latent space. 2023. 1, 2
- [28] Edwin H Land and John J McCann. Lightness and retinex theory. *Josa*, 61(1):1–11, 1971. 2
- [29] Zhengqi Li and Noah Snavely. Cgintrinsics: Better intrinsic image decomposition through physically-based rendering. In *ECCV*, 2018. 2
- [30] Zhengqi Li, Ting-Wei Yu, Shen Sang, Sarah Wang, Meng Song, Yuhan Liu, Yu-Ying Yeh, Rui Zhu, Nitesh Gundavarapu, Jia Shi, et al. Openrooms: An open framework for photorealistic indoor scene datasets. In *CVPR*, pages 7190–7199, 2021. 2
- [31] Zhengqi Li, Jia Shi, Sai Bi, Rui Zhu, Kalyan Sunkavalli, Miloš Hašan, Zexiang Xu, Ravi Ramamoorthi, and Manmohan Chandraker. Physically-based editing of indoor scene lighting from a single image. In *ECCV*, pages 555–572. Springer, 2022. 2, 3, 6, 8
- [32] Haohe Liu, Zehua Chen, Yi Yuan, Xinhao Mei, Xubo Liu, Danilo Mandic, Wenwu Wang, and Mark D Plumbley. Audioldm: Text-to-audio generation with latent diffusion models. *arXiv preprint arXiv:2301.12503*, 2023. 2

- [33] Jundan Luo, Zhaoyang Huang, Yijin Li, Xiaowei Zhou, Guofeng Zhang, and Hujun Bao. Niid-net: adapting surface normal knowledge for intrinsic image decomposition in indoor scenes. *IEEE TVCG*, 26(12):3434–3445, 2020. 2
- [34] Chenlin Meng, Yutong He, Yang Song, Jiaming Song, Jiajun Wu, Jun-Yan Zhu, and Stefano Ermon. Sdedit: Guided image synthesis and editing with stochastic differential equations. In *ICLR*, 2021. 1, 2
- [35] Ron Mokady, Amir Hertz, Kfir Aberman, Yael Pritch, and Daniel Cohen-Or. Null-text inversion for editing real images using guided diffusion models. *arXiv*, 2022. 1, 2
- [36] Puntawat Ponglertnapakorn, Nontawat Tritrong, and Supasorn Suwajanakorn. Difareli: Diffusion face relighting. *arXiv preprint arXiv:2304.09479*, 2023. 2, 3, 4, 6, 8
- [37] Zia-ur Rahman, Daniel J Jobson, and Glenn A Woodell. Multi-scale retinex for color image enhancement. In *ICIP*, pages 1003–1006. IEEE, 1996. 4
- [38] Robin Rombach, Andreas Blattmann, Dominik Lorenz, Patrick Esser, and Björn Ommer. High-resolution image synthesis with latent diffusion models. In *CVPR*, 2022. 1, 2
- [39] Olaf Ronneberger, Philipp Fischer, and Thomas Brox. U-net: Convolutional networks for biomedical image segmentation. In *MICCAI*, 2015. 3
- [40] Steven A Shafer. Using color to separate reflection components. *Color Research & Application*, 10(4):210–218, 1985. 3
- [41] Jascha Sohl-Dickstein, Eric Weiss, Niru Maheswaranathan, and Surya Ganguli. Deep unsupervised learning using nonequilibrium thermodynamics. In *ICML*, 2015. 3
- [42] Jiaming Song, Chenlin Meng, and Stefano Ermon. Denoising diffusion implicit models. In *ICLR*, 2021. 4, 5, 7
- [43] Yang Song, Conor Durkan, Iain Murray, and Stefano Ermon. Maximum likelihood training of score-based diffusion models. *NeurIPS*, 34:1415–1428, 2021. 3
- [44] Yang Song, Jascha Sohl-Dickstein, Diederik P Kingma, Abhishek Kumar, Stefano Ermon, and Ben Poole. Score-based generative modeling through stochastic differential equations. In *ICLR*, 2021. 3
- [45] Guy Tevet, Sigal Raab, Brian Gordon, Yonatan Shafir, Daniel Cohen-Or, and Amit H Bermano. Human motion diffusion model. *arXiv preprint arXiv:2209.14916*, 2022. 2
- [46] Weicai Ye, Shuo Chen, Chong Bao, Hujun Bao, Marc Pollefeys, Zhaopeng Cui, and Guofeng Zhang. Intrinsicnerf: Learning intrinsic neural radiance fields for editable novel view synthesis. In *Proceedings of the IEEE/CVF International Conference on Computer Vision*, pages 339–351, 2023. 2
- [47] Fisher Yu, Yinda Zhang, Shuran Song, Ari Seff, and Jianxiong Xiao. Lsun: Construction of a large-scale image dataset using deep learning with humans in the loop. In *ARXIV*, 2015. 5
- [48] Chong Zeng, Yue Dong, Pieter Peers, Youkang Kong, Hongzhi Wu, and Xin Tong. Dilightnet: Fine-grained lighting control for diffusion-based image generation. In *ACM SIGGRAPH 2024 Conference Proceedings*, 2024. 2
- [49] Zheng Zeng, Valentin Deschaintre, Iliyan Georgiev, Yannick Hold-Geoffroy, Yiwei Hu, Fujun Luan, Ling-Qi Yan, and Miloš Hašan. Rgb \leftrightarrow x: Image decomposition and synthesis using material-and lighting-aware diffusion models. *arXiv preprint arXiv:2405.00666*, 2024. 2
- [50] Lvmin Zhang, Anyi Rao, and Maneesh Agrawala. Adding conditional control to text-to-image diffusion models. In *Proceedings of the IEEE/CVF International Conference on Computer Vision*, pages 3836–3847, 2023. 1, 2
- [51] Xiuming Zhang, Pratul P Srinivasan, Boyang Deng, Paul Debevec, William T Freeman, and Jonathan T Barron. Nerfactor: Neural factorization of shape and reflectance under an unknown illumination. *ACM TOG*, 40(6):1–18, 2021. 2
- [52] Rui Zhu, Zhengqin Li, Janarбек Matai, Fatih Porikli, and Manmohan Chandraker. Irisformer: Dense vision transformers for single-image inverse rendering in indoor scenes. In *CVPR*, pages 2822–2831, 2022. 2, 3

Retinex-Diffusion: On Controlling Illumination Conditions in Diffusion Models via Retinex Theory

Supplementary Material

A. Cross Color Ratios

Section 4.3 introduced one can use cross color ratios to represent part of the illumination-invariant components. Here we provide the detail to prove the CCR is illumination-invariant. Taking the logarithm on both side of the Equation (11), we get:

$$\log M_{RG} = \log R_{p_1} + \log G_{p_2} - \log R_{p_2} - \log G_{p_1}. \quad (14)$$

Given the image formation in Equation (1) and [4], at certain point, we obtain:

$$C_{p_1} = m_b(\mathbf{n}, \mathbf{s})e^{C_{p_1}(\lambda)}\rho_b^{C_{p_1}(\lambda)} + m_s(\mathbf{n}, \mathbf{s}, \mathbf{v})e^{C_{p_1}(\lambda)}\rho_s^{C_{p_1}(\lambda)}, \quad (15)$$

where C_{p_1} represents the color channel C at pixel p_1 , for an input image. ρ_b and ρ_s represent the body diffuse reflectance and specular reflectance respectively. Since the two neighbouring pixels p_1 and p_2 , the same illumination condition can be assumed. Therefore,

$$e^{C_{p_1}} = e^{C_{p_2}}. \quad (16)$$

Then, Equation (12) can be derived. It is important to note that the Cross-Color Ratio (CCR) is solely influenced by the surface reflectance. Consequently, the CCR remains invariant to changes in illumination.